

TiO₂ deactivation during gas-phase photocatalytic oxidation of ethanol

Eva Piera, José A. Ayllón, Xavier Doménech, José Peral*

Departament de Química, Edifici Cn, Universitat Autònoma de Barcelona, 08193 Bellaterra (Cerdanyola del Vallès), Spain

Abstract

The deactivation of TiO₂ Degussa P25 during the gas-phase photocatalytic oxidation of ethanol has been studied. Water vapor plays a clear competitive role for surface sites adsorption, thus hampering the ethanol photo-oxidation. Dark adsorption of ethanol on a fresh catalyst shows a Langmuirian behavior with the formation of a monolayer of adsorbate. Dark adsorption in a TiO₂ surface that has been used in consecutive photocatalytic experiments of ethanol degradation gives non-Langmuirian isotherms, indicating the existence of noticeable changes of the catalyst surface structure. After several irradiations the catalyst activity decreases. Such deactivation has been investigated, observing that the rate constant of ethanol and acetaldehyde (its main degradation product) oxidation decreases with irradiation time. Several surface treatments have been studied in order to find suitable procedures for catalytic activity recovery, but regular decay of activity is always observed after every treatment. © 2002 Elsevier Science B.V. All rights reserved.

Keywords: TiO₂; Photocatalysis; Ethanol

1. Introduction

The gas-phase photocatalytic oxidation of organic contaminants is a subject of current interest due to its potential for removal of low concentration pollutants in slightly contaminated enclosed atmospheres (closed intelligent buildings, factory buildings, especially enclosed atmospheres, etc.). Previous work can be found where the advantages and drawbacks of the photocatalytic technique are highlighted, especially when compared to photocatalytic processes in aqueous phase [1–3]. In particular, (i) the reaction mechanisms in the gas phase seem to be different to those that prevail in aqueous systems, and (ii) relatively low levels of UV light energy are needed for the occurrence of

gas-phase processes, in contrast to reactions in water [4]. In the gas phase, decomposition rates have been found extremely high, making the technique very useful for practical applications [1,5–7]. Gas-phase reactions also allow the direct application of analytical tools to monitor the composition, structure and electronic states of substrate and adsorbates, and hence, reaction mechanisms could be directly elucidated [8]. Jardim et al. [9] have mentioned additional advantages: (a) the diffusion of reagents and products is favored; (b) HO• scavengers present in water phase such chlorides or alkalinity do not interfere; (c) electron scavengers such as O₂ are rarely limiting; (d) photons absorbed by air are low.

Despite all these advantages gas-phase photocatalysis presents an important drawback. While in aqueous phase water helps to remove reaction intermediates and reaction products from the catalyst surface (specially those compounds of polar character), in gas

* Corresponding author. Tel.: +34-93-581-2772;
fax: +34-93-581-2920.
E-mail address: jose.peral@uab.es (J. Peral).

phase these species tend to accumulate in the surface causing the deactivation of the catalyst. This phenomenon has already been elegantly described by Sauer and Ollis [10] and in other previous works [11–13]. Thus gas-phase TiO_2 deactivation needs to be studied in detail if the technique is to be of practical application.

In the present paper deactivation of TiO_2 Degussa P25 during the photocatalytic degradation of ethanol is studied and several procedures of catalyst activity recovery are examined.

2. Experimental

The experimental setup used in this study is shown in Fig. 1. Dry synthetic air is supplied with a compressed air tank (1), the flow being carefully controlled with an electronic gas flowmeter (2). This allowed the buildup of a desired pressure of air inside the recirculation loop. The loop was constructed with stainless steel tube and contained a gas reservoir tank (6), the photoreactor (4), a recirculating pump (9), a gas

chromatograph (8), and several valves (3) that allow the system to operate in continuous or recirculation modes.

The method used to operate the system was as follows: once the loop (total volume: 1067 ml) was filled with dry air from the tank the required amount of ethanol and water were injected in the inlet port (7) located at the gas reservoir. The pump was turned on (flow rate: 375 ml min^{-1}) and a moderate time was allowed to pass to ensure liquid water and ethanol evaporation. Chromatographic analysis were performed to determine the final ethanol gas-phase concentration, allowing the assessment of ethanol dark adsorption. Once the system was equilibrated the light was turned on and the change in ethanol, acetaldehyde and CO_2 concentrations were monitored. In a regular experiment $0.16 \mu\text{l}$ of ethanol were injected in the reservoir; this produced a theoretical (ignoring ethanol adsorption on the catalyst) gas-phase ethanol concentration of 118 mg m^{-3} .

The cylindrical photocatalytic reactor (4) (6.7 cm high and 6.60 cm^2 of illuminated area) had a quartz window that allowed UV illumination from the

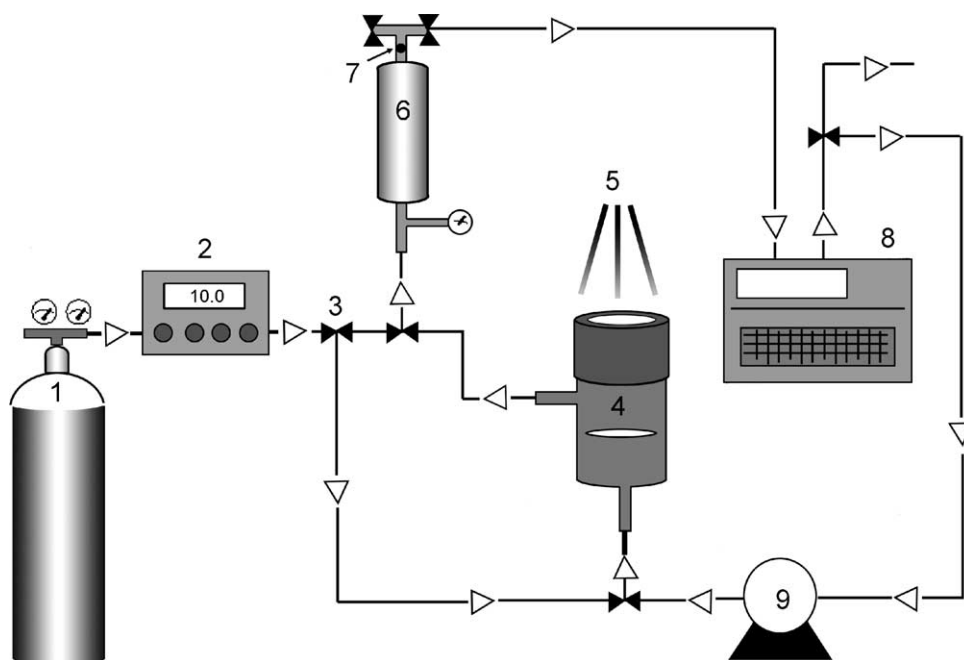


Fig. 1. Experimental setup: (1) dry air tank; (2) mass flow controller; (3) three port valves; (4) photoreactor; (5) light source; (6) gas reservoir; (7) injection port; (8) gas chromatograph; (9) recirculating pump.

top. An amount of 10.7 mg of the powdered catalyst was spread on top of an attached fritted glass plate perpendicular to the light beam. The inlet and outlet ports were placed in a way that the gas was forced to cross the catalyst film. The photoreactor is similar to the one employed by Peral and Ollis [11]. A 80 W Friolite HB medium pressure mercury lamp was used as light source (5); the irradiation energy arriving at the top of the catalyst was $143.5 \mu\text{W cm}^2$, measured with a UV radiometer (Lutron UVA 365) centered at 365 nm.

The gas-phase composition was monitored by using a gas chromatograph (8) (Varian Star 3400 Cx) equipped with a Porapack Q column and two detectors: a flame ionization detector (FID) used to follow the concentration of ethanol and acetaldehyde, and a thermal conductivity detector (TCD) used to follow concentrations of CO_2 and H_2O . The detection of acetic acid was carried out by solid–liquid extraction and a consequent GC–MS analysis with a HP 6890 gas analyzer equipped with a HP5 (5% phenyl) column and connected to a HP 5973 mass spectrometer.

The ethanol used in the experiments was Panreac (more than 99.8% purity with a maximum water content of 0.02%). Thirty three percent of H_2O_2 aqueous solutions (Panreac) were used in the activity recovery experiments. The water injected was of Milli-Q grade. The TiO_2 used was Degussa P25 (80% anatase, 20% rutile, BET surface area of $59.1 \text{ m}^2 \text{ g}^{-1}$, average particle size of 27 nm).

3. Results and discussion

The photo-oxidation of gas-phase ethanol in presence and absence of water vapor was carried out in order to ascertain the effect that water concentration has on the reaction rate. Around 118 mg m^{-3} of ethanol were injected in the gas reservoir, the gas reached dark adsorption equilibrium with the fresh catalyst surface (10.7 mg TiO_2) leaving a gas-phase ethanol concentration of 48 mg m^{-3} . Thus, 0.119 mg m^{-2} of ethanol adsorbed onto the TiO_2 surface. Once the dark adsorption equilibrium was reached light was turned on and the ethanol concentration decreased with irradiation time. Sauer and Ollis [14] have identified acetaldehyde, formaldehyde and CO_2 as intermediate and reaction products of ethanol photo-oxidation, and

have justified the presence of acetic acid and formic acid with a theoretical kinetic network model, while Nimlos et al. [15] and Muggli et al. [16] have identified acetaldehyde, formaldehyde, acetic acid and formic acid as intermediate products for the same photocatalytic process. Due to experimental limitations only gas-phase acetaldehyde and CO_2 have been quantitatively detected in the present work. A solid–liquid extraction (TiO_2 –water) of the used TiO_2 catalyst and a GC–MS analysis of the liquid phase revealed the presence of acetic acid adsorbed on the TiO_2 surface.

Fig. 2a shows the dependence of the square root of ethanol concentration with time in absence of water and in the presence of approximately 100% relative humidity (26400 mg m^{-3} of water). As can be seen, the data fits a straight line in both cases ($r^2 = 0.996$ in the absence of water, and $r^2 = 0.994$ in the presence of water). This simple fitting contrasts with the complex mathematical model elaborated by Sauer and Ollis [14], where a Langmuir–Hinshelwood kinetic with competitive adsorption of five species (ethanol, acetaldehyde, formaldehyde, acetic acid, and formic acid) on two different adsorption sites is considered. The authors presented a modeling of the time course of all species involved, with r^2 for the curve fitting of ethanol and acetaldehyde species of 0.73 and 0.7, respectively. In contrast, the half-order fitting gives a much simplified situation, with a closer approach to the quantitative behavior of ethanol and acetaldehyde. A half-order fitting could be theoretically explained with a Langmuir–Hinshelwood kinetic where the adsorption of ethanol takes place with simultaneous dissociation and occupancy of two surface sites, being the competition of the reaction intermediates for adsorption sites negligible. In fact, if Sauer's data is conveniently analyzed (see, for example, Figs. 4 and 6 of [14]) an excellent linear behavior between the square root of concentration and time is obtained ($r^2 > 0.99$). The case of ethanol adsorption with simultaneous dissociation is reasonable taking into account that ethanol has a weak acid character. The existence of two different surface sites for ethanol adsorption on TiO_2 , pointed out by Sauer and Ollis [14], and confirmed by Nimlos et al. [15] and Pilkenton et al. [17], is also in agreement with the dissociation of ethanol in two separated fragments.

Fig. 2b shows data corresponding to acetaldehyde photo-oxidation. Acetaldehyde concentration has the

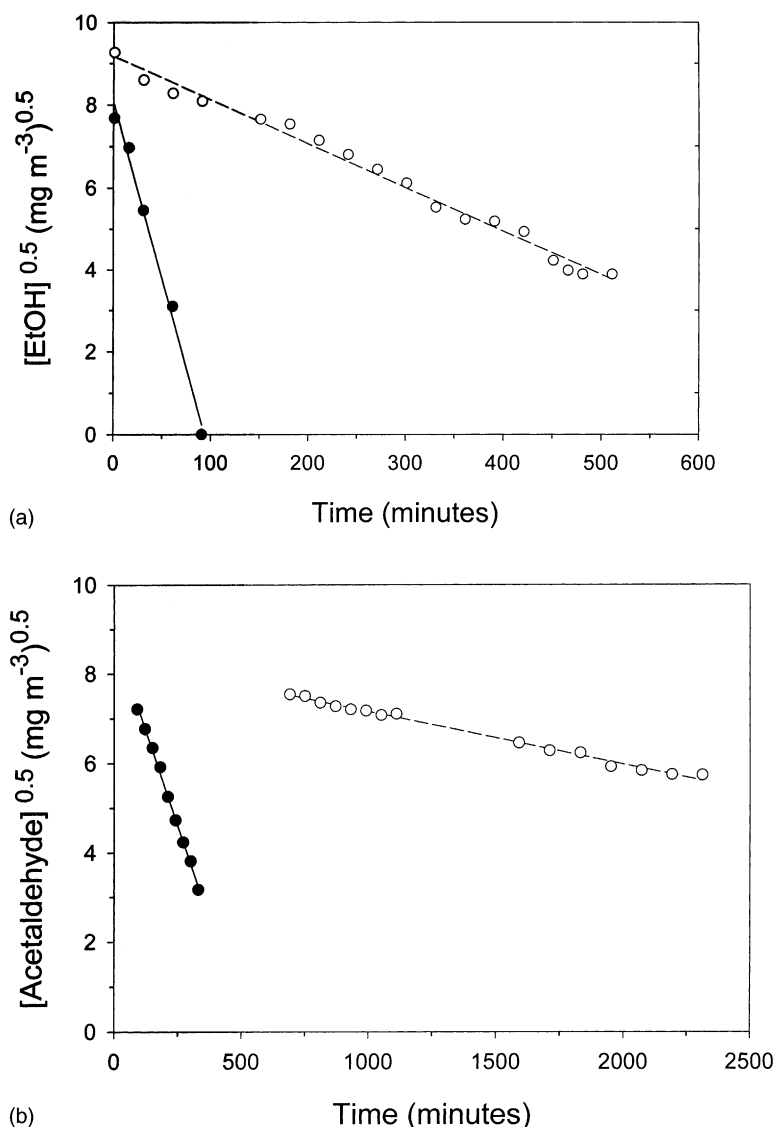


Fig. 2. Square root of ethanol (a) and acetaldehyde (b) concentrations vs. time for experiments in the absence (●) and presence (○) of water (118 mg m^{-3} of ethanol, and $26\,400 \text{ mg m}^{-3}$ of water were injected).

typical dependence with time expected for a reaction intermediate (see Fig. 4), going from zero to a maximum value and again to zero. The data shown in Fig. 2b corresponds to acetaldehyde concentration after passing the maximum in the same experiment of ethanol photo-oxidation of Fig. 2a. Again, an excellent linear regression ($r^2 = 0.997$) between the square root of concentration and time is obtained. However,

for acetaldehyde it is difficult to discuss the results in terms of simultaneous adsorption and dissociation, since the hydrogen of the aldehyde group is not acidic. Muggli et al. [18] studied the photo-oxidation of acetaldehyde and they assumed a first-order kinetics of acetaldehyde removal.

Table 1 contains the reaction rate constants of ethanol and acetaldehyde degradation considering a

Table 1

Reaction rate constants (k) of ethanol and acetaldehyde disappearance in presence and absence of water^a

Relative humidity (%)	Ethanol k ($\text{mg m}^{-3} \text{ min}^{-1}$) ^{0.5}	Acetaldehyde k ($\text{mg m}^{-3} \text{ min}^{-1}$) ^{0.5}
0	0.086 ± 0.012	0.017 ± 0.001
100	0.0106 ± 0.0008	0.00118 ± 0.00008

^a Constants deduced from data in Fig. 2.

half-order reaction, both, in presence and absence of water. As can be seen, a 100% humidity clearly makes the process more difficult, while the ethanol degradation is inherently faster than the acetaldehyde one.

The presence of water clearly deactivates the photo-oxidation of ethanol and acetaldehyde. In steady-state experiments, Falconer and Magrini-Bair [19] have shown that water displaces both ethanol and acetaldehyde from the catalyst surface. Thus, the slow decrease of both reactant concentration can be attributed to adsorption competition. Since the main interest of this work was to study catalyst surface deactivation during ethanol photo-oxidation, the decision was taken not to inject water in the original

gas mixture. On the other hand, the presence of water is unavoidable, since water is a product of ethanol mineralization.

Since catalyst deactivation is related to reactant adsorption capability, experiments were carried out where the dark adsorption of ethanol in a reused catalyst (catalyst that was used during several complete cycles of ethanol photocatalysis) was quantified. Fig. 3 shows the dark adsorption isotherms of ethanol in a catalyst that has been reused six times. As can be inferred from the figure data analysis, just after the first photocatalytic run ($[\text{ethanol}]_0 = 118 \text{ mg m}^{-3}$, reaction time 500 min; after this reaction time no organics remained in gas phase) the dark adsorption decreases from 0.119 mg m^{-2} of ethanol (fresh catalyst) to 0.0697 mg m^{-2} (catalyst used once). Thus, there is a 43% decrease of ethanol dark adsorption. Taking into account that the experiment was carried out with 10.7 mg of TiO_2 and that the total gas volume was 1067 ml , the number of molecules adsorbed on the fresh catalyst and on the catalyst used one time are 10^{18} and 5.7×10^{17} , respectively. Assuming a surface site concentration on TiO_2 of

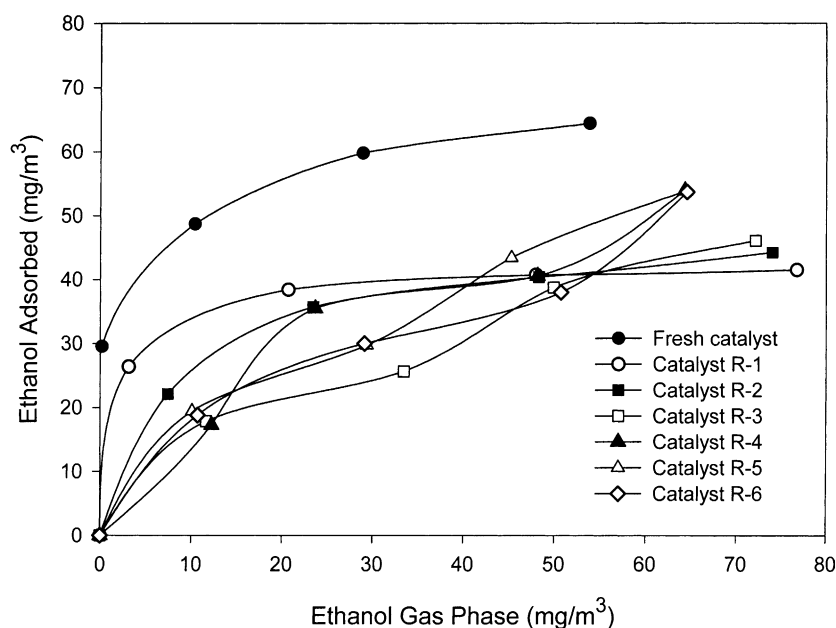


Fig. 3. Dark adsorption isotherms of ethanol in a TiO_2 that has been used in six consecutive photocatalytic experiments. The isotherm data was collected in the dark periods between photocatalysis (118 mg m^{-3} of ethanol injected for each irradiation). Reaction time 500 min (complete removal of gas-phase organics). The legend inside the figure refers to the number of times the catalyst has been used.

5.0×10^{14} sites cm^{-2} [20], the total available number of sites is 2.5×10^{18} , which means that, there are 2.5 more sites than ethanol molecules adsorbed on the saturated fresh catalyst. Considering that ethanol seems to need two adsorption sites in order to participate in a dissociative adsorption, 80% of the surface sites would be covered during the reactant adsorption. The remaining 20% would probably be occupied by water molecules, or it can just be due to uncertainties on the total number of surface sites available.

For the rest of the adsorption experiments, with the catalyst used up to six times in photocatalytic experiments, no Langmuirian isotherms are observed. The shape of these isotherms seems to indicate that the catalyst surface undergoes profound modification during photocatalysis. Since a Langmuirian (monolayer) adsorption is observed for the fresh catalyst and the catalyst used just one time, it seems reasonable to think that ethanol can adsorb on top of some of the organic deposits responsible for deactivation after several runs. Peral and Ollis [13] have suggested that the species responsible for permanent deactivation of the TiO_2 are

of carbonaceous nature. If that is the case, adsorption of ethanol onto carbon sites should be thermodynamically feasible and could explain the existence of different adsorption sites on the catalyst surface, and the non-Langmuirian nature of the isotherms.

In order to study the catalyst deactivation, data of the photocatalytic experiments conducted between the adsorption experiments presented above was collected. Figs. 4 and 5 show the time course of ethanol, acetaldehyde and CO_2 during the first (fresh catalyst) and the sixth run (catalyst reused five times). As can be seen, with a fresh catalyst gas-phase ethanol concentration decreases with time, being negligible after 100 min of irradiation. During that period acetaldehyde concentration is building up, reaching a maximum just at the moment that ethanol disappears. At that time, gas-phase CO_2 also seems to form. The fact that gas-phase acetaldehyde clearly reacts when ethanol has disappeared has also been observed by Sauer and Ollis [14], and it points towards a competition between the two species for the same adsorption sites, as suggested by Muggli et al. [16]. During

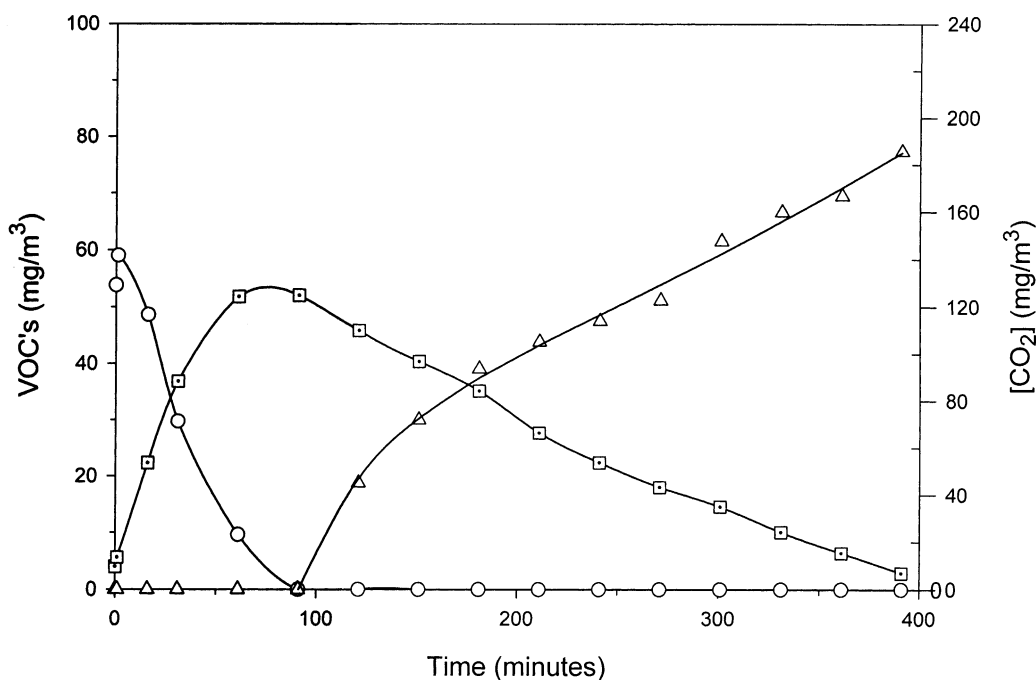


Fig. 4. Time course of ethanol (○), acetaldehyde (◻) and CO_2 (Δ) during the first experiment of ethanol photocatalysis (fresh catalyst) with the TiO_2 used for the dark adsorption experiments of Fig. 3.

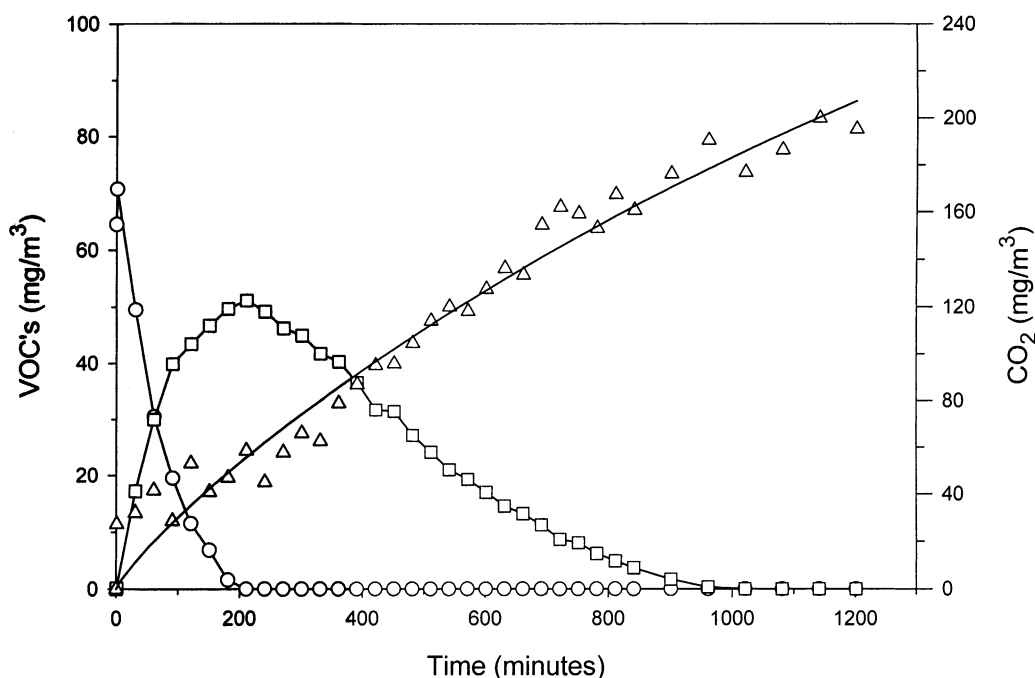


Fig. 5. Time course of ethanol (○), acetaldehyde (□) and CO₂ (Δ) during the sixth experiment of ethanol photocatalysis (catalyst reused six times) with the TiO₂ used for the dark adsorption experiments of Fig. 3.

the following 300 min, acetaldehyde concentration decreases, almost going to zero, while CO₂ concentration keeps growing. After 400 min of reaction, with no ethanol and acetaldehyde present in gas phase, the mass balance is not closed. Around 180 mg m⁻³ of CO₂ are present, while a maximum of 225.7 mg m⁻³ should be expected after complete ethanol mineralization was achieved. Hence, part of the initial organic carbon is still adsorbed on the catalyst surface at the end of the experiment. The adsorbed species clearly interferes with the following ethanol photo-oxidation runs. Fig. 5 shows that the time needed to achieve a complete elimination of gas-phase ethanol in the sixth run is around 200 min. Again, acetaldehyde oxidation only begins when gas-phase ethanol has disappeared. In this case CO₂ is detected in gas phase from the beginning of the reaction, due to the mineralization of the organic species remaining in the catalyst surface at the end of the previous experiment. The time needed for complete destruction of acetaldehyde goes now to almost 1000 min, and the CO₂ concentration reaches a value close to 200 mg m⁻³, which is not yet

the stoichiometric CO₂ concentration expected after ethanol mineralization. Hence, more reaction intermediates remain in the catalyst surface after each consecutive run. It is interesting to note that the initial gas-phase ethanol concentration is larger in the sixth run, although the same amount of ethanol was injected for each experiment, probably due to partial catalyst surface coverage by the organic remains of the previous run and partial displacement of ethanol. After the six irradiations the TiO₂ acquires a permanent pale yellow color, indicating the presence of carbonaceous deposits on its surface.

Table 2 contains the reaction rate constants of ethanol and acetaldehyde photo-oxidation of the several consecutive experiments of photocatalysis carried out between the consecutive dark adsorption experiments shown in Fig. 3 (only initial rate values of ethanol and acetaldehyde disappearance were considered). As can be seen, there is a clear reduction of the rate constants for both species with an increasing number of runs, indicating the existence of catalyst deactivation. It has been previously shown [21] that

Table 2

Reaction rate constants (k) of ethanol and acetaldehyde disappearance in the photocatalytic experiments performed between the dark adsorption experiments of Fig. 3

Experiment	Time ^a (min)	Ethanol k ($\text{mg m}^{-3} \text{min}^{-1}$) ^{0.5}	Acetaldehyde k ($\text{mg m}^{-3} \text{min}^{-1}$) ^{0.5}
Fresh TiO_2	0	0.086 ± 0.012	0.017 ± 0.001
TiO_2 R-1	400	0.072 ± 0.007	0.014 ± 0.001
TiO_2 R-2	800	0.059 ± 0.004	0.011 ± 0.001
TiO_2 R-3	1200	0.051 ± 0.003	0.011 ± 0.001
TiO_2 R-4	1600	0.047 ± 0.003	0.0103 ± 0.0004
TiO_2 R-5	2000	0.040 ± 0.004	0.0097 ± 0.0005
TiO_2 R-6	2400	0.036 ± 0.003	0.0089 ± 0.0004

^a Time the catalyst had already been exposed to light at the beginning of each experiment.

the phenomena of heterogeneous catalyst deactivation can be quantified with an experimental equation like

$$\frac{k}{k_0} = \frac{1}{1 + t^b} \quad (1)$$

where t is the time of use of the catalyst, k_0 the initial reaction rate constant obtained with a fresh catalyst, k the observed reaction rate constant at time t , and b is an adjustable experimental parameter that directly depends on the nature of the oxidized substrate. The rate constants of Table 2 have been used to check the usefulness of Eq. (1) in this study. Because the rate constants correspond to consecutive experiments with the same catalyst they have been referred to the time passed since the fresh catalyst was first used (see column 2 in Table 2, $t = \sum$ time of each run). For long reaction time, Eq. (1) can be approximated to

$$\frac{k}{k_0} \approx \frac{1}{t^b} \quad (2)$$

and taking logarithms:

$$\ln k = \ln k_0 + b \ln t \quad (3)$$

thus, $\ln k$ should be a linear function of $\ln t$ with b being the slope of the corresponding straight line. With the values of $\ln k$ and $\ln t$ of Table 2, linear regressions for ethanol and acetaldehyde are obtained with b equal to 0.37 and 0.24, respectively. From Eq. (2) it is obvious that a larger b value implies a faster deactivation. Thus the deactivation caused by ethanol is faster than the one due to acetaldehyde. The experimental behavior of the present system seems to be in accordance with previous observed experimental deactivations.

Several surface treatments were examined in order to recover the catalyst activity. The treatments were performed with the same TiO_2 sample, and a set of photocatalytic experiments (see Fig. 7 for the exact number of irradiations) were carried out between each catalyst recovery treatment. In this way, further deactivation of the treated catalyst could also be studied. The treatments were as follows:

- *Treatment 1*: Catalyst exposed to 15 h continuous flow of pure air under UV irradiation.
- *Treatment 2*: 24 h exposure of the catalyst to a clean recirculating air atmosphere with approximately 100% and relative humidity with simultaneous UV irradiation.
- *Treatment 3*: 56 h exposure of the catalyst to a recirculating air atmosphere that contains a vaporized H_2O_2 solution ($343 \text{ mg m}^{-3} \text{H}_2\text{O}_2$ and $800 \text{ mg m}^{-3} \text{H}_2\text{O}$) and simultaneous UV irradiation.
- *Treatment 4*: 24 h exposure of the catalyst to a recirculating air atmosphere that contains a vaporized H_2O_2 solution ($1030 \text{ mg m}^{-3} \text{H}_2\text{O}_2$ and $2403 \text{ mg m}^{-3} \text{H}_2\text{O}$) and simultaneous UV irradiation.
- *Treatment 5*: Catalyst exposed to 24 h continuous flow of pure air at 80°C and under UV irradiation.
- *Treatment 6*: Catalyst exposed to 24 h continuous flow of pure air at 150°C and under UV irradiation.
- *Treatment 7*: 24 h exposure of the catalyst to a recirculating air atmosphere that contains a vaporized H_2O_2 solution ($1373 \text{ mg m}^{-3} \text{H}_2\text{O}_2$ and $3204 \text{ mg m}^{-3} \text{H}_2\text{O}$) and simultaneous UV irradiation.
- *Treatment 8*: 48 h exposure of the catalyst to a recirculating air atmosphere that contains a vaporized H_2O_2 solution ($1373 \text{ mg m}^{-3} \text{H}_2\text{O}_2$ and $3204 \text{ mg m}^{-3} \text{H}_2\text{O}$) at 150°C and simultaneous UV irradiation, plus 48 h exposure of the catalyst to a recirculating air atmosphere that contains a vaporized H_2O_2 solution ($1373 \text{ mg m}^{-3} \text{H}_2\text{O}_2$ and $3204 \text{ mg m}^{-3} \text{H}_2\text{O}$) at room temperature and simultaneous UV irradiation.
- *Treatment 9*: Catalyst previously soaked with $40 \mu\text{l}$ of the H_2O_2 solution (the solution is distributed onto the catalyst by using a micropipette) and exposed to a clean air atmosphere during 24 h and under UV irradiation.

Table 3

Experimental conditions of the different treatments carried out for catalyst recovery^a

Treatment number	Treatment time (h)	Gas phase	Operation mode	Temperature
1	15	Clean air	Continuous flow	Room temperature
2	24	100% relative humidity	Recirculation	Room temperature
3	56	343 mg m ³ of H ₂ O ₂	Recirculation	Room temperature
4	24	1030 mg m ³ H ₂ O ₂	Recirculation	Room temperature
5	24	Clean air	Continuous flow	80 °C
6	24	Clean air	Continuous flow	150 °C
7	24	1030 mg m ³ of H ₂ O ₂	Recirculation	Room temperature
8	48 + 48	1030 mg m ³ of H ₂ O ₂	Recirculation	150 °C + room temperature
9	24	Clean air ^b	Continuous flow	Room temperature

^a All the treatments were carried out under UV irradiation.^b The TiO₂ had been previously soaked with 40 µl of a 33% H₂O₂ solution.

Table 3 summarizes the main features of the different treatments. It is important to keep in mind that a series of photocatalytic runs were carried out between each catalyst recovery treatment (see Fig. 7 for the photocatalytic experiments details). The recovery of the catalyst dark adsorption should reflect the recovery of activity, if any. Thus, Fig. 6 shows the maximum

amount of ethanol adsorbed on the TiO₂ surface after each treatment (it is important to remember here that the treatments are consecutively applied to the same catalyst sample).

Several remarks can be made from data in Fig. 6. Although treatment 1 seems to recover all the surface adsorption sites this is just due to the relatively mild

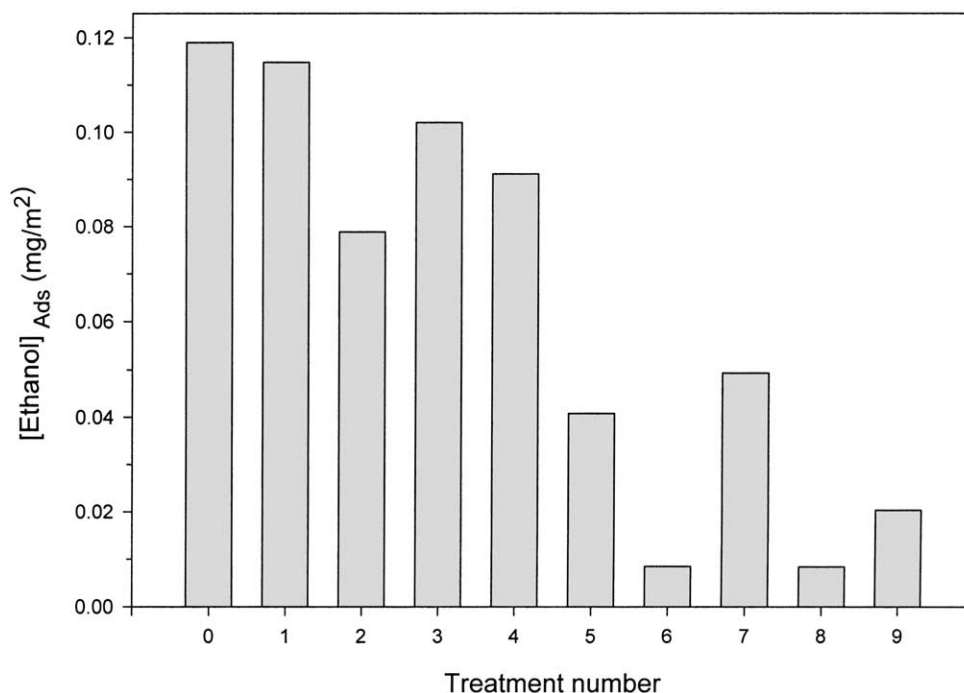


Fig. 6. Maximum ethanol adsorbed (when a constant plateau is achieved at the corresponding adsorption isotherm) onto a TiO₂ sample that is successively used in photocatalytic experiments and treatment processes designed to recover the catalyst activity (see Table 3 for experimental details).

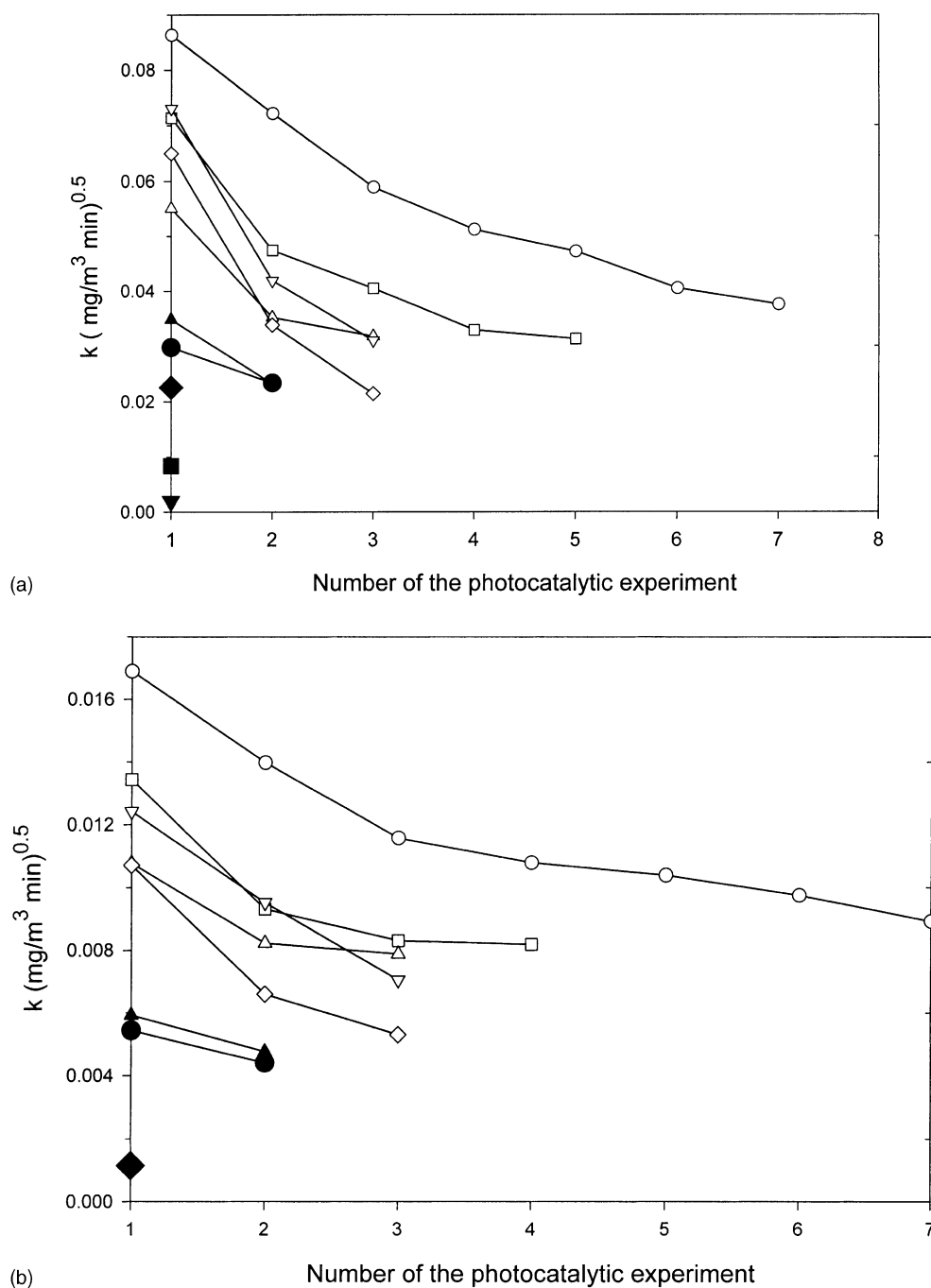


Fig. 7. Decay of the reaction rate constants of ethanol (a) and acetaldehyde (b) photocatalytic oxidation for consecutive experiments carried out with the same TiO_2 sample. After the corresponding series of photocatalytic experiments the catalyst was submitted to the regeneration treatments specified in Table 3: untreated catalyst (○); after treatment 1 (□); after treatment 2 (△); after treatment 3 (▽); after treatment 4 (◇); after treatment 5 (●); after treatment 6 (■); after treatment 7 (▲); after treatment 8 (▼); after treatment 9 (◆). All the experiments shown in this figure were performed with the same TiO_2 sample.

deactivation that the catalyst had suffered at that time. Several cycles of catalyst use and treatment with this procedure show continuous decrease of ethanol adsorption (data not shown). The combination of clean air and irradiation only partially recovers the surface activity, as shown by Peral and Ollis [11]. Although water adsorption is mainly reversible, the presence of water during treatment 2 clearly hampers the surface recovery, due to the role of water as competitor for surface sites. Temperature is also opposed to the recovery of surface adsorption and as can be seen, the catalyst treated at 150 °C (treatment 6) almost completely loses its ethanol adsorption capability. This can only be explained by considering that temperature helps the thermocatalytic conversion of some of the intermediates remaining in the surface after photocatalysis (e.g. acetaldehyde) to a less volatile and thus, more enduring and deactivating species (e.g. acetic acid). In this way, temperature seems to accelerate the process of formation of the carbonaceous deposits, a process that on the other hand, appears to be unavoidable. The use of a relatively powerful oxidant like H₂O₂ partially recovers the ethanol surface adsorption, but this is never the one observed for the fresh catalyst. Treatment 4 uses a larger amount of oxidant, but the adsorption recovery is lower than in treatment 3, indicating that catalyst surface deactivation cannot be completely avoided. Treatment 9 supports this assertion because it uses a more drastic approach: the catalyst is wetted with a H₂O₂ solution, but the surface recovery is only minor because the treatment is the last one after the long series of deactivation and recovery experiments.

The fact that the deactivation persists after the different treatments is clearly observed in Fig. 7 where the reaction rate constant of consecutive experiments of photocatalytic degradation of ethanol and acetaldehyde are shown. The catalyst treatments described in Table 3 and the consequent irradiation series of Fig. 7 were done with the same TiO₂ sample. Even in those cases where the catalyst activity recovery after surface treatment is effective (e.g. after treatments 3, 4 and 7) the activity always decays in consecutive photocatalytic experiments. It is important to notice that the activity decay of the TiO₂ after treatment 1 is faster than the decay observed for the fresh catalyst (compare the initial slopes of the curves with open circles (○) and open squares (□) in Fig. 7a and b). Also, the

first reaction rate constant after treatment 1 is clearly lower than the first reaction rate constant with the fresh catalyst, something that cause surprise since adsorption of ethanol in the fresh and the treated catalyst is almost the same (as seen in Fig. 6 for treatment 0 and 1). There is a clear trend in the system reactivity towards a complete passivation, no matter what number and type of recovery treatment is applied. At the end of the series of experiments the reaction rate constants are almost zero for both ethanol and acetaldehyde. Some treatments seem to produce a partial activity recover.

In this sense the use of H₂O₂ (treatments 3, 4, 7 and 9) gives a noticeable increase of the first photocatalytic reaction rate constant when compared to reaction rate constant of the corresponding previous treatment, but even in those cases the photocatalytic activity rapidly decreases in consecutive irradiation experiments. All the experimental evidence points toward the formation of surface species that are not easily removed with the surface treatment procedures proposed in this study.

4. Conclusions

The deactivation of TiO₂ Degussa P25 during gas-phase photocatalytic oxidation of ethanol has been studied. Dark adsorption of ethanol onto a fresh catalyst follows a Langmuirian isotherm, but the adsorption features change when the catalyst sample is reused in several photocatalytic runs. Changes on the surface chemical nature are suggested by the adsorption isotherm shapes, probably due to ethanol adsorption onto the carbonaceous deposits responsible for catalyst deactivation. Ethanol and acetaldehyde disappearance have been found to follow a half-order kinetics and the presence of water seriously hampers the process. The deactivation process has been quantified using an experimental equation. Several surface treatments have been tested but it was always impossible to completely recover the initial ethanol dark adsorption and photocatalytic reactivity. The treatment of the surface with temperatures between 80 and 150 °C is highly detrimental because it accelerates the formation of the deactivating deposits. In any case, the catalyst activity goes down no matter what number and type of surface treatment were tried.

Acknowledgements

The authors thank the Spanish Ministry of Science and Technology (Project PB98-011) and the CYTED network VIII-G for supporting this study.

References

- [1] E. Berman, J. Dong, in: W.W. Eckenfelder, A.R. Bowen, J.A. Roth (Eds.), *Proceedings of the Third International Symposium on Chemical Oxidation: Technology for the Nineties*, Technomic Publishers, Chicago, 1993, pp. 183–189.
- [2] J. Peral, X. Domènech, D.F. Ollis, *J. Chem. Technol. Biotechnol.* 70 (1997) 117.
- [3] R.M. Alberici, W.F. Jardim, *Appl. Catal. B: Environ.* 14 (1997) 55.
- [4] L.A. Dibble, G.B. Raupp, *Environ. Sci. Technol.* 26 (1992) 492.
- [5] M. Murabayashi, K. Itoh, K. Togashi, K. Shiozawa, H. Yamazaki, *J. Adv. Oxid. Technol.* 4 (1999) 71.
- [6] S. Yamazaki-Nishida, K.J. Nagano, L.A. Phillips, S. Cervera-March, M.A. Anderson, *J. Photochem. Photobiol. A: Chem.* 70 (1993) 95.
- [7] G.B. Raupp, C.T. Junio, *Appl. Surf. Sci.* 72 (1993) 321.
- [8] J.C. Hemminger, R. Carr, G.A. Somorjai, *Chem. Phys. Lett.* 57 (1978) 100.
- [9] W.F. Jardim, R.M. Alberici, M.M.K. Takiyama, C.P. Huang, *Hazard. Ind. Wastes* 26 (1994) 230.
- [10] M.L. Sauer, D.F. Ollis, *J. Catal.* 163 (1996) 215.
- [11] J. Peral, D.F. Ollis, *J. Catal.* 136 (1992) 554.
- [12] J. Peral, D.F. Ollis, in: D.F. Ollis, H. Al-Ekabi (Eds.), *Photocatalytic Purification and Treatment of Water and Air*, Elsevier, Amsterdam, 1993, pp. 741–745.
- [13] J. Peral, D.F. Ollis, *J. Mol. Catal.* 115 (1997) 347.
- [14] M.L. Sauer, D.F. Ollis, *J. Catal.* 158 (1996) 570.
- [15] M.R. Nimlos, E.J. Wolfrum, M.L. Brewer, J.A. Fennell, G. Bintner, *Environ. Sci. Technol.* 30 (1996) 3102.
- [16] D.S. Muggli, J.T. McCue, J.L. Falconer, *J. Catal.* 173 (1998) 470.
- [17] S. Pilkenton, S. Hwang, D. Raftery, *J. Phys. Chem. B* 103 (1999) 11152.
- [18] D.S. Muggli, K.H. Lowery, J.L. Falconer, *J. Catal.* 180 (1998) 111.
- [19] J.L. Falconer, K.A. Magrini-Bair, *J. Catal.* 179 (1998) 171.
- [20] L.P. Childs, D.F. Ollis, *J. Catal.* 66 (1980) 383.
- [21] H.S. Fogler, *Elements of Chemical Reaction Engineering*, Prentice-Hall, New York, 1986, pp. 273–274.